COBEM 2021 26th International Congress of Mechanical Engineering
November 22-26, 2021, Virtual Congress, Brazil
ABCM Associação Brasileira de Engenharia e Ciências Mecânicas

COB-2021-1806
NUMERICAL INVESTIGATION OF THE DESTRUCTIVE INTERFERENCE OF TWO NONLINEAR STANDING WAVES IN A DUCT

Guilherme Mendes Santana
Roberto Francisco Bobenrieth Miserda
Adriano Todorovic Fabro
Universidade de Brasília, Campus Universitário Darcy Ribeiro, Brasília, DF - 70910-900
santana.mendes@aluno.unb.br
rfbm@unb.br
fabro@unb.br

Abstract. *This work aims at investigating the interaction of high amplitude sound waves generated in opposing phases in a closed duct. This paper presents four numerical studies of propagation and interaction of sound waves in a one-dimensional duct. The cases are studied using the numerical solution of the Euler equations for a compressible flow, with finite volumes domain discretization, fluxes calculated with fourth-order precision and a third-order Runge-Kutta scheme for the time march. The sound waves are generated by the movement of walls at the extremities of the domain. The boundary conditions are imposed with a moving-body, immersed-boundary method, and an interpolation inside the control volumes was proposed to properly capture the movement of the walls. The simulation of sound waves that interact inside a closed duct, a resonant cavity, showed the formation of linear and nonlinear standing waves, depending on the amplitude of the sound waves. Based on the analysis of the interaction of two sound waves with opposing phases, it is shown that as the intensity of the sound increases, the noise cancellation efficacy is reduced. Moreover, the simulation of the continuous interaction of sound waves inside the cavity showed that for high amplitudes, the system eventually reaches an equilibrium between the energy input from the generation of the sound waves and the energy loss caused by the shock waves formed due to the nonlinear effects, and the pressure fluctuations remain approximately constant. The results agree with the theory of nonlinear acoustics and point out that the proposed approach can properly simulate such nonlinear sound waves interaction.*

Keywords: *Computational aeroacoustics, Nonlinear acoustics, Acoustic resonators, Immersed boundary method, Inviscid flow*

1. INTRODUCTION

Nonlinear acoustics is the field of acoustics concerned with studying sound waves with large amplitudes. The nonlinear effects that influence these waves can be divided into two categories, as described by Lighthill (1956). One category contemplates the thermodynamic irreversibilities associated with viscous effects and heat transfer, while the other includes the change in the speed of sound due to the pressure fluctuations and the advective transport of the wave by the flow induced by the wave itself. The present work will focus on the effects of the latter category.

Even though linear acoustics is an adequate tool to describe sound waves in several applications, there are situations in which the nonlinear effects cannot be disregarded. On some aeroacoustics problems, for example, such as the noise generation in aircraft engines, sound waves have very high amplitudes, and it is possible that the nonlinear effects are important. Therefore, the comprehension of the influence of the nonlinear effects on the propagation and interaction of sound waves can lead to a better understanding of several aeroacoustics problems.

Thus, the objective of this work is to investigate the influence of the nonlinear effects on the shape of sound waves and on the interaction of sound waves with opposing phases inside a closed, one-dimensional duct. The interaction of the waves with opposing phases in the closed duct should result in a standing wave and the interaction of two standing waves with opposing phases should result in completely destructive interference, in the absence of nonlinear effects. Therefore, these cases highlight the influence of the nonlinear effects.

1.1 Governing Equations

The flow of air will be modelled by the one-dimensional Euler equations for a compressible flow, the continuity equation (Eq. (1)), the momentum equation, (Eq. (2)) and the energy equation (Eq. (3)),

$$\frac{\partial \rho}{\partial t} + \frac{\partial (\rho u)}{\partial x} = 0, \tag{1}$$

$$\frac{\partial (\rho u)}{\partial t} + \frac{\partial (\rho u u)}{\partial x} = -\frac{\partial p}{\partial x} + \rho f_x, \tag{2}$$

and

$$\frac{(\partial \rho e_t)}{\partial t} + \frac{\partial (\rho u e_t)}{\partial x} = \frac{\partial (p\, u)}{\partial x} + \rho u f_x, \tag{3}$$

as well as the constitutive equations for an ideal and thermally perfect gas,

$$p = \rho\, R\, T, \tag{4}$$

and

$$e_t = c_v\, T, \tag{5}$$

where u is the velocity, ρ is the density, p is the pressure, f_x represents the body forces, e_t is the total energy, R is the gas constant, T is the temperature and c_v is the specific heat at constant volume.

1.2 Numerical Method

This system of nonlinear partial differential equations is solved numerically with a finite volumes domain discretization, a fourth-order precision scheme for the calculation of the fluxes, and a third-order Runge-Kutta scheme for the time march. The boundary conditions at the extremities of the duct will be applied with a moving body immersed boundary method. This numerical method is described in detail by Miserda *et al.* (2020).

In the present work, the sound waves that propagate in the closed duct are generated by the oscillatory movement of the walls at the extremities, and the boundary conditions are directly applied to the finite volumes that contain the boundary points through a moving body immersed boundary method. Due to the small time step and to the small amplitude of the movement of the walls necessary to generate the sound waves, the walls remain in the same control volume for several time steps. As a consequence, because the mean values of the properties in the control volumes are used to apply the boundary conditions, variation of the position of the wall does not influence the flow. Figure 1 illustrates how the boundary remains in the same control volumes for several consecutive time steps. It is worth mentioning that, even though the change of position does not influence the flow, the velocity of the wall changes with time and influences the flow.

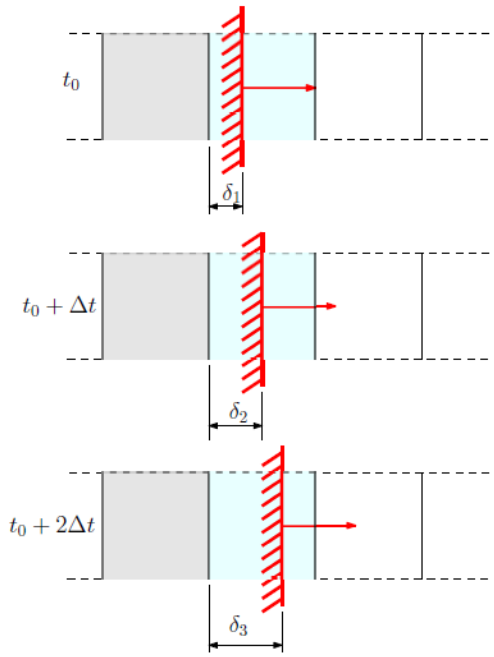

Figure 1: Movement of the boundary inside the control volume.

To better capture the movement of the wall, a variation of the original method presented by Miserda *et al.* (2020) is proposed in this work. Instead of directly using the mean values of the properties in the neighboring control volumes, the values of the properties over the surfaces of the control volumes are first calculated with the fourth-order precision scheme used for the fluxes. Then, new values for the properties in the control volumes are calculated with a linear interpolation inside each control volume, based on the distance δ, as shown in Fig. 2.

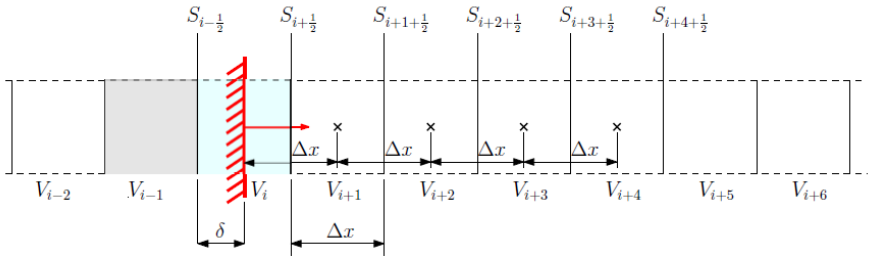

Figure 2: Adaptation of the immersed boundary method.

Thus, the value of the density interpolated inside the control volume V_{i+1} is calculated as

$$\rho^*_{i+1} = \rho_{i+\frac{1}{2}} + \frac{\delta\left(\rho_{i+1+\frac{1}{2}} - \rho_{i+\frac{1}{2}}\right)}{\Delta x}, \tag{6}$$

where $\rho_{i+\frac{1}{2}}$ is the density calculated over surface $S_{i+\frac{1}{2}}$, which separates volumes V_i and V_{i+1}, $\rho_{i+1+\frac{1}{2}}$ is the density calculated over surface $S_{i+1+\frac{1}{2}}$ which separates volumes V_{i+1} an V_{i+2}, Δx is the size of the control volume, δ is the distance between the boundary and the left surface of the control volume and the superscript $*$ indicates that the value is calculated with the linear interpolation inside the control volume.

1.3 Methodology

To investigate the influence of nonlinear effects on the propagation and interaction of sound waves, the present work is divided into four cases, or configurations of simulations. For each case, sound waves of different intensities are analyzed aiming at comparing the approximately linear waves with the clearly nonlinear waves. The first case (presented in Section 2.1) consisted of the study of plane waves that propagate in a duct with an open extremity. The waves are generated by the oscillatory movement of the wall on the extremity of the duct.

The second case (presented in Section 2.2) consisted of the analysis of standing waves that form in a closed duct when the length of the duct is proportional to the frequency of the sound wave, i.e., $f = n\,a/2\,L$, where f is the frequency of the wave, a is the velocity of sound and L is the length of the duct. In this case, one of the walls moves to generate sound waves while the other remains static, and reflects the wave. Thus, the emitted and reflected waves interact to form the standing wave. After the standing wave is established, the wall movement is interrupted.

The third case (presented in Section 2.3) consisted of the study of the interaction of two standing waves with opposing phases. In this case, both walls emitted sound waves and reflected the waves emitted by the opposing wall, which resulted in the two standing waves with opposing phases. As in the second case, after the two standing waves are formed and interact completely, the movement of the walls is interrupted.

The fourth case (presented in Section 2.4) consisted of the study of the continuous interaction of sound waves. In this case, both walls oscillated through the entire simulation, and sound waves were continuously emitted into the duct.

For cases one, three an four, the velocity of the walls, v is given by

$$v\,(t) = A\,2\pi\,f\,\sin^3\left(2\pi\,f\,t\right), \tag{7}$$

where A is the amplitude of the movement and is the parameter associated to the intensity of the sound waves, f is the frequency of the movement of the walls and t is the time. Equation 7 was chosen to ensure that the beginning and the end of the wall movement is smooth, i. e., both velocity and acceleration are zero at the beginning and end of the movement. For case 2, the velocity of the walls is given by

$$v\,(t) = A\,2\pi\,f\,\sin\left(2\pi\,f\,t\right), \tag{8}$$

even though the use of Eq. 8 implies that the movement of the walls starts and ends with maximum acceleration.

For all cases, different values for the amplitude A of the movement were used to compare linear and nonlinear cases. In addition to that, for all cases the frequency of the movement of the walls was $f = 1000$ Hz.

2. RESULTS

2.1 Plane Waves Propagating on an Open Duct

The first case studied in the present work was the propagation of sound waves on a duct with an open extremity. Figure 3a shows the pressure as a function of time at different positions along the duct, for an amplitude of oscillation of the wall of $1,0 \times 10^{-8}$ m. This results in a sound wave with a sound pressure level of 57 dB, which corresponds to the noise level of a normal conversation. These graphics show that, for this amplitude, there is no significant change to the shape of the wave which indicates that the nonlinear effects are not relevant in this case.

Figure 3b shows the results for the pressure as a function of time at the same positions along the duct as Fig. 3a, for an amplitude of oscillation of the wall of $7,0 \times 10^{-4}$ m. This results in a sound pressure level (SPL) of 154 dB, which can cause permanent hearing loss in humans even for small exposure times. In this case, the deformation of the wave by the nonlinear effects is clearly visible. In the compression region, the temperature is higher, and the velocity of propagation is also higher, and the flow induced by the sound wave is in the same direction of propagation of the wave. In the expansion region, on the other hand, the temperature and the velocity of sound are smaller and the induced flow is in the opposite direction of the propagation of sound. The consequence of these differences is that the peaks propagate faster than the valleys, and the wave is distorted as shown in the graphics. When this distortion is large enough, the sound wave acquires a saw-tooth shape.

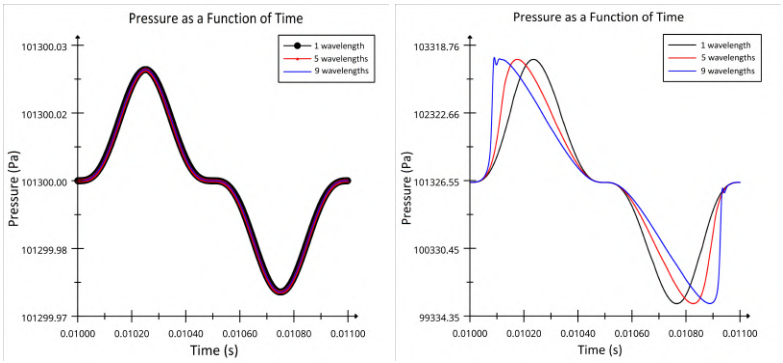

(a) Amplitude 10^{-8} m. (b) Amplitude $7,0 \times 10^{-4}$ m.

Figure 3: Pressure signal for different distances from the source.

2.2 Standing Waves Formed in a Closed Duct

The second case consisted of the analysis of standing waves that form when waves with opposing propagation directions interact. Figure 4 shows the linear standing pressure wave, associated with a wall movement amplitude of 10^{-8} m. For this case, the wave keeps the sinusoidal form throughout the entire simulation and does not show signs of distortion due to nonlinear effects.

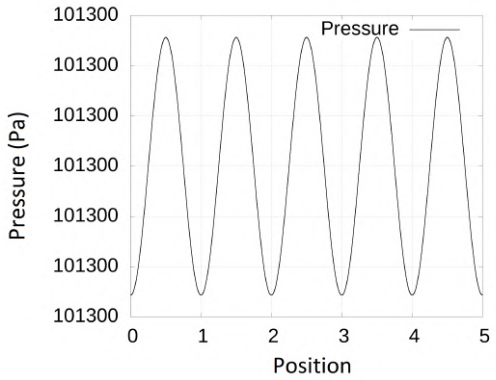

Figure 4: Linear standing wave.

Figure 5 shows the nonlinear standing pressure wave, associated to a wall movement amplitude of 10^{-4} m. Figure 5a shows the standing wave at time $t = 0.0105$ s. In this instant, the wave still has an approximately sinusoidal form, because there was not enough time for the difference in the propagation velocity to influence the shape of the wave. However, the results in Fig. 5b, at $t = 0.0505$ already shows some distortion in the shape of the wave, which indicates that, at this

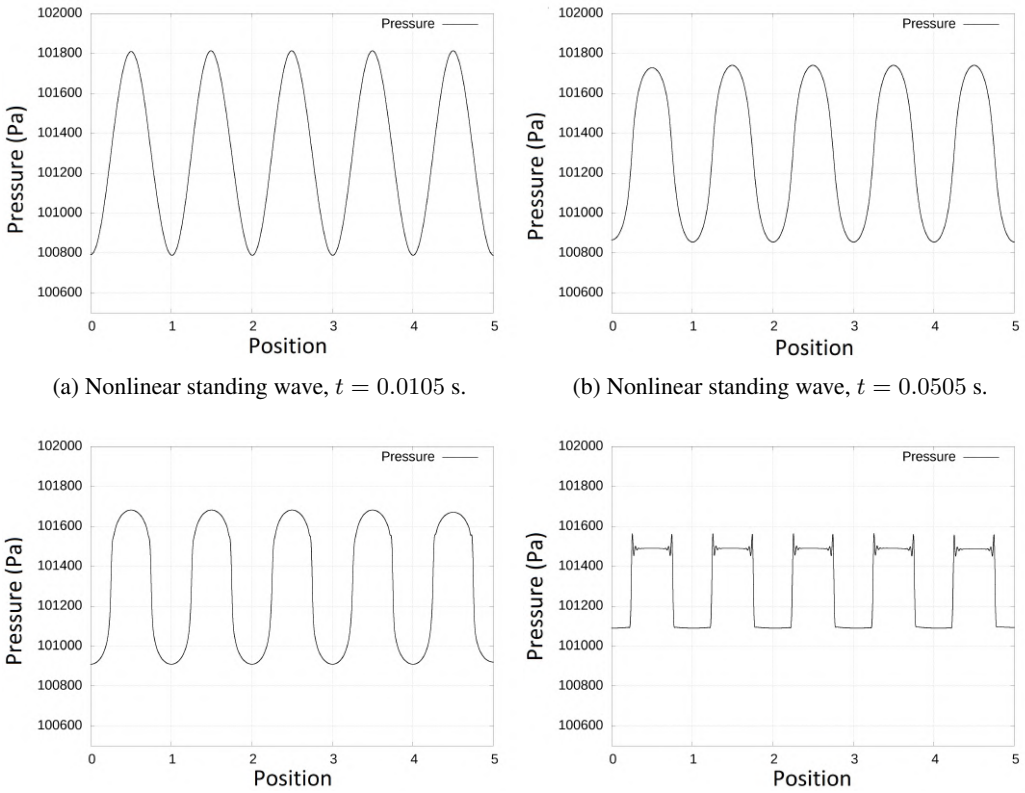

(a) Nonlinear standing wave, $t = 0.0105$ s.

(b) Nonlinear standing wave, $t = 0.0505$ s.

(c) Nonlinear standing wave, $t = 0.0755$ s.

(d) Nonlinear standing wave, $t = 0.2255$ s.

Figure 5: Pressure distribution of the nonlinear standing wave at different time instants.

moment, the nonlinear effects have started to influence the sound waves. The results for the standing wave at $t = 0.0755$ s, in Fig. 5c shows that the nonlinear effects cause the appearance of regions with very high pressure gradients. Figure 5d shows that, at time $t = 0.2255$, the nonlinear effects have resulted in the formation of shock waves.

2.3 Interaction of Standing Waves With Opposing Phases

After observing how the nonlinear effects influence the sound waves and the standing waves, the interaction between two standing waves was studied. For each amplitude of the movement of the walls, the average sound pressure level throughout the duct was calculated. These results and those for the sound pressure level associated with the plane waves are presented in Fig. 6.

Figure 6 indicates that up to a wall movement amplitude of 10^{-6} m, there is an approximately constant noise level reduction of about 41 dB, and both curves remain parallel. This behavior indicates that, for small amplitudes, the standing waves are approximately symmetric, not deformed by the nonlinear effects, and the interaction results in destructive interference. However, for increasing amplitudes of the wall movement, the noise reduction starts to decrease. This indicates that the nonlinear effects are breaking the symmetry of the standing waves, as previously shown, and the destructive interference is less effective in reducing noise levels. It can also be noticed that, from an amplitude of $2,0 \times 10^{-4}$ m on, there appears to be an increase in the sound pressure level reduction. This effect is not due to destructive interference between the standing waves. In fact, for these higher amplitudes, the nonlinear effects cause the appearance of shock waves, as in Fig. 3b, and the irreversibilities associated with the shock cause a reduction of the amplitude of the pressure fluctuations.

2.3.1 Wall Movement Amplitude of 10^{-8} m

The results in Fig. 7 show the pressure fields inside the duct at different time instants, until the complete interaction of the sound waves, for an amplitude of the wall movement of 1,0 $\times 10^{-8}$. Figure 7f shows that, even after the complete interaction of the sound waves, there are small pressure fluctuations, which indicate that even for very small amplitudes, the destructive interference is not complete.

Figure 8 shows the results of the pressure signals at the start of the interaction between the sound waves (Fig 8a) and after the interaction (Fig. 8b). These results also show that there is some pressure fluctuation after the interaction, even though the amplitude is much smaller.

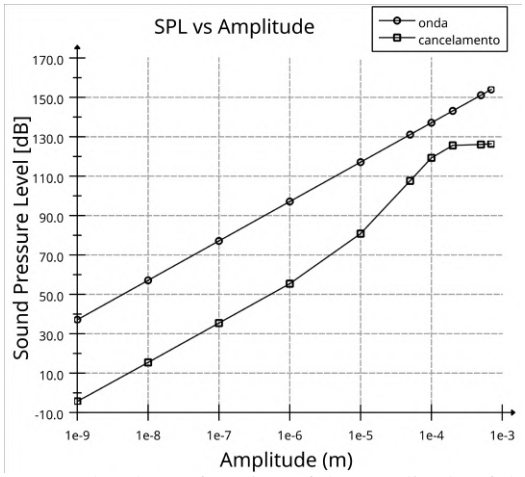

Figure 6: Sound pressure level as a function of the amplitude of the wall movement.

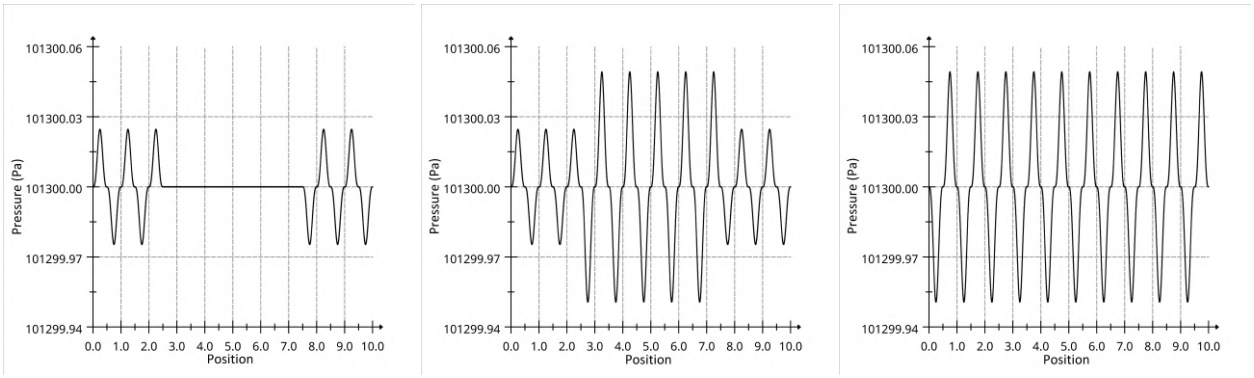

(a) $t = 0,0025$ s. (b) $t = 0,0075$ s. (c) $t = 0,01$ s.

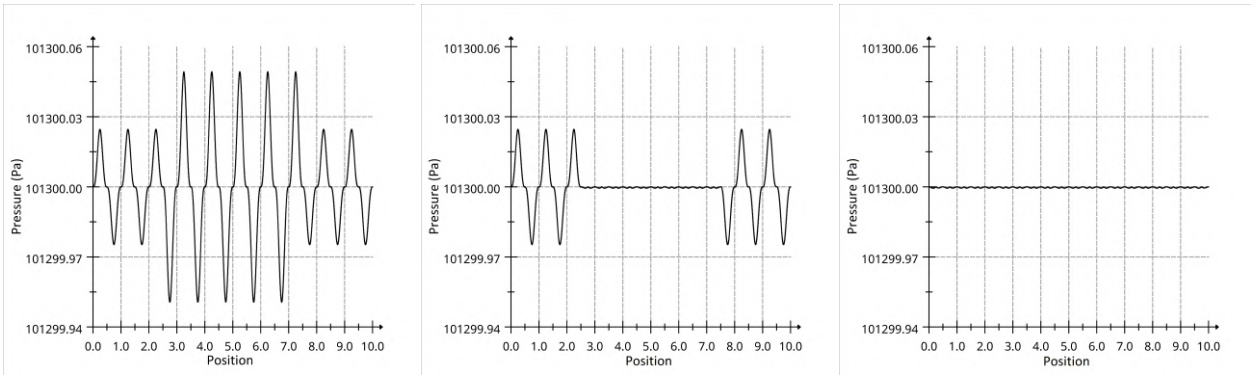

(d) $t = 0,0125$ s. (e) $t = 0,0175$ s. (f) $t = 0,0205$ s.

Figure 7: Evolution of the pressure field, wall movement amplitude of 10^{-8} m.

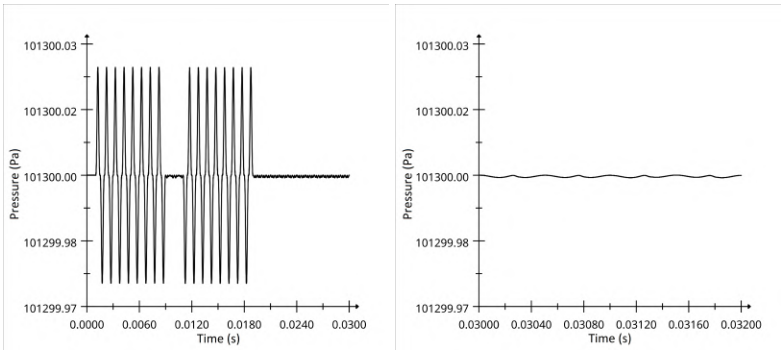

(a) Initial interval. (b) After the complete interaction.

Figure 8: Pressure signals, wall movement amplitude of 10^{-8} m.

2.3.2 Wall Movement Amplitude of 10^{-4} m

Figure 9 shows the pressure fields inside the duct for different time instants for a wall movement with amplitude of 10^{-4} m. These results show a reduced effect of the destructive interference, due to the nonlinear effects breaking the symmetry between the expansion and compression phases of the sound wave.

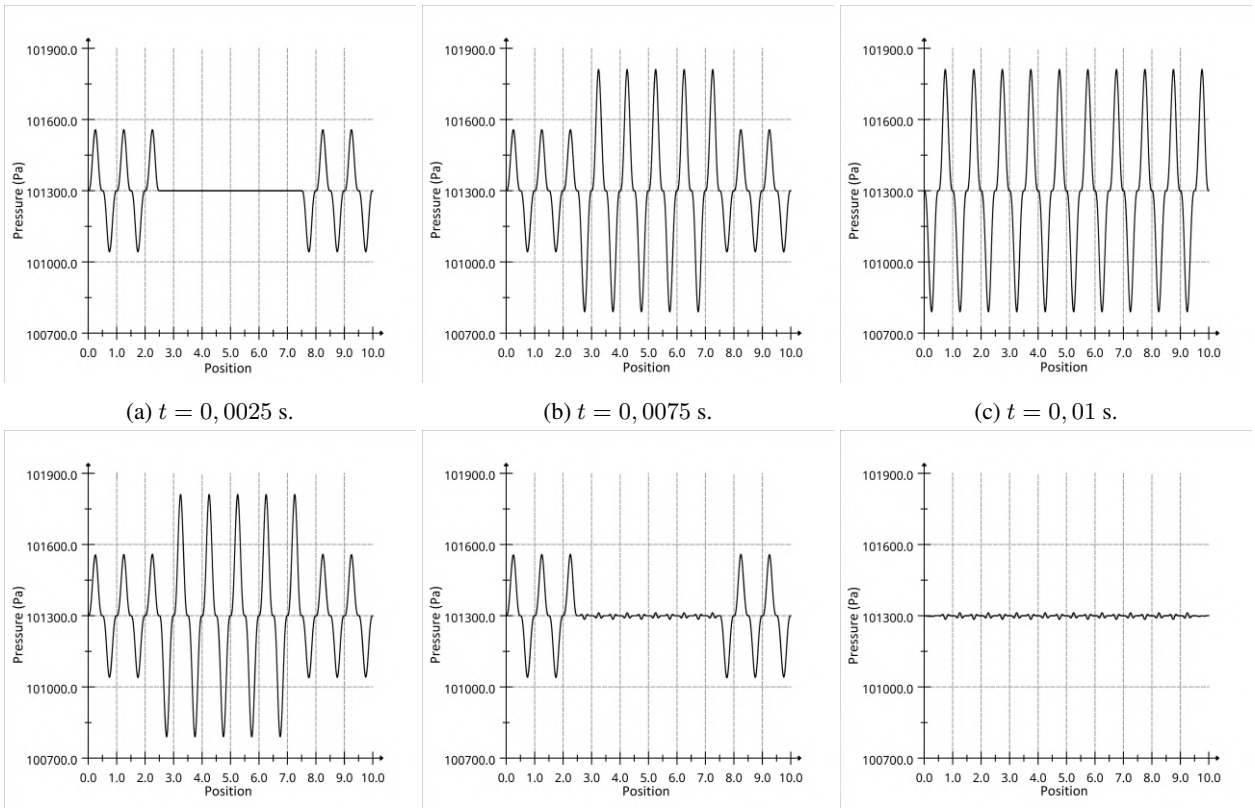

(a) $t = 0,0025$ s. (b) $t = 0,0075$ s. (c) $t = 0,01$ s.

(d) $t = 0,0125$ s. (e) $t = 0,0175$ s. (f) $t = 0,0205$ s.

Figure 9: Evolution of the pressure field, wall movement amplitude of 10^{-4} m.

The results if Fig. 10 show the pressure signals at the start of the interaction between the waves (Fig. 10a) and after the interaction (Fig. 10b). These results, as well as the pressure fields in Fig. 9, show that there is a significantly higher pressure fluctuation because the change in propagation velocity breaks the symmetry of the sound waves.

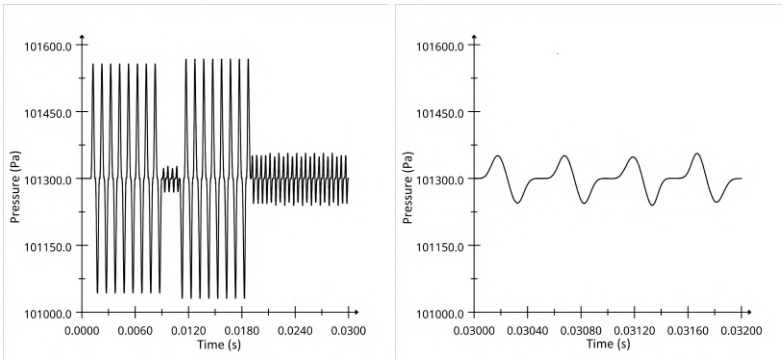

(a) Initial phase. (b) After complete interaction.

Figure 10: Pressure signals, wall movement amplitude of 10^{-4} m.

2.4 Continuous Interaction of Sound Waves in a Closed Duct

The final case studied in the present work was the flow induced by the continuous oscillation of the walls at the extremities of the duct. This case is motivated by the fact that it is not common to interrupt the noise generation before the analysis, as happened in the previous cases. Figure 11a shows the envelope of the pressure fluctuations, for a wall

movement amplitude of 1.0×10^{-3} m. This higher amplitude was used without the appearance of shock waves by reducing the length of the duct to one wavelength of the undisturbed sound wave.

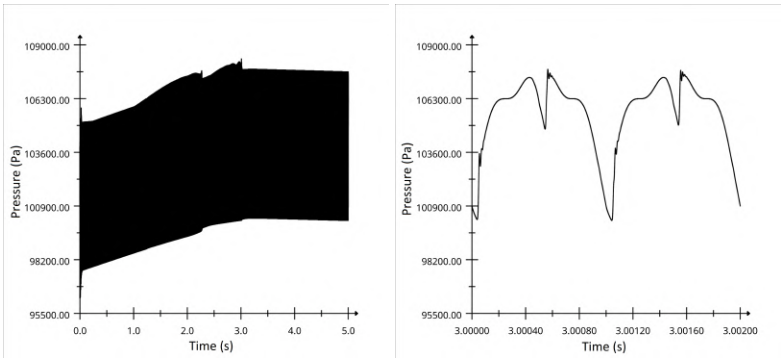

(a) Pressure fluctuations envelope. (b) Pressure fluctuation at $t = 3.0$ s.

Figure 11: Continuous interaction of sound waves, wall movement amplitude of 10^{-3} m.

Figure 11a shows that there is a moment, at approximately $t = 3.0$ s when the amplitude of the wave acquires an approximately constant value. At this point, it is possible that there is an equilibrium between the energy input due to the movement of the walls and the energy loss due to the irreversibility of the shock wave. Figure 11b shows the shock waves that cause the equilibrium starting around $t = 3.0$ s.

3. CONCLUSIONS

In the present work, several numerical simulations were conducted of the flow induced by the oscillatory movement of walls, that act as sound sources. To better capture the movement of these walls, the moving body immersed boundary method described by Miserda *et al.* (2020) was modified with a linear interpolation scheme inside the control volumes. The simulations of the plane wave showed that the influence of the nonlinear effects on the shape of the sound waves depends on the distance from the sound source, and this influence is compatible with the theoretical description by Lighthill (1956). The simulations of the standing waves revealed that the strategy of using a static wall to reflect the sound waves does cause the emitted and reflected waves to interact and form standing waves, but it is necessary to interrupt the movement of the wall when the standing wave is formed. The result for the linear standing wave is compatible with the expected results from linear acoustics. The result for the nonlinear standing waves also agrees well with results from nonlinear acoustics theory (Enflo and Hedberg, 2002). The analysis of the interaction of two standing waves with opposing phases showed that, for small amplitudes, there is a significant reduction in sound pressure level, which indicates that the symmetry of the waves results in destructive interference. However, it was possible to observe that, even for small amplitudes, there are residual pressure fluctuations, which indicates that nonlinear effects influence even waves with a small, but finite, amplitude. This is compatible with the idea presented by Gurbatov *et al.* (2011), according to whom any periodic oscillation in a nondissipative medium is influenced by the nonlinear effects, and eventually acquires a saw-tooth shape.

4. REFERENCES

Enflo, B.O. and Hedberg, C.M., 2002. *Theory of Nonlinear Acoustics in Fluids*. Kluwer Academic Publishers.

Gurbatov, S., Rudenko, O. and Saichev, A., 2011. *Waves and Structures in Nonlinear Nondispersive Media*. Springer.

Lighthill, M.J., 1956. "Viscosity effects in sound waves of finite amplitude". *Surveys in Mechanics*, pp. 250–351. Eds. G. K. Batchelor and R. M. Davies (Cambridge University Press).

Miserda, R.F.B., Pimenta, B.G. and da Rocha, L.S., 2020. "Numerical simulation of rotor-stator interaction noise in transonic cascades". *Journal of Propulsion and Power*, Vol. 36, No. 3, pp. 363–380. doi:10.2514/1.B37627. URL `https://doi.org/10.2514/1.B37627`.

5. RESPONSIBILITY NOTICE

The authors are solely responsible for the printed material included in this paper.